EPJ Web of Conferences **2**, 14002 (2010)
DOI:10.1051/epjconf/20100214002

Influence Of The Neutron Richness On Binary Decays

G. Ademard[1,a], J.P. Wieleczko[1], E. Bonnet[1], A. Chbihi[1], J.D Frankland[1], M. La Commara[2], M. Vigilante[2], E. Rosato[2], A. D'Onofrio[3], G. Spadaccini[2], J. Gomez del Campo[4], C. Beck[5], B. Borderie[6], R. Bougault[7], R. Dayras[8], G. De Angelis[9], A. Galindo-Uribarri[4], P. Lautesse[10], N. Le Neindre[7], M. Parlog[7], D. Pierroutsakou[2], F. Rejmund[1], M.F. Rivet[6], M. Romoli[11], R. Roy[12], and D. Shapira[4]

[1] GANIL, CEA et IN2P3-CNRS, B.P. 55027, F-14076, Caen Cedex, France
[2] Dipartimento di Scienze Fisiche, Università di Napoli "Federico II", I 80126, Napoli, Italy
[3] Dipartimento di Scienze Ambiantali, Università di Napoli, I 81100, Caserta, Italy
[4] Physics Division, Oak Ridge National Laboratory, Oak Ridge, TN 37831, USA
[5] IPHC, IN2P3-CNRS, F 67037, Strasbourg Cedex2, France
[6] IPNO, IN2P3-CNRS and Université Paris-Sud 11, F-91406, Orsay Cedex, France
[7] LPC, IN2P3-CNRS, ENSICAEN and Université, F-14050, Caen Cedex, France
[8] CEA, IRFU, SPhN, CEA/Saclay, F-91191, Gif sur Yvettes Cedex, France
[9] NFN, LNL, I 35020 Legnaro (Padova) Italy
[10] IPNL, IN2P3-CNRS et Université, F-69622, Villeurbanne Cedex, France
[11] Dipartimento di Scienze Fisiche, Università di Napoli "Federico II", I 81100, Caserta, Italy
[12] Laboratoire de Physique Nucléaire, Université de Laval, Québec, Canada

Abstract. The influence of the neutron richness on binary decays is investigated in ^{78,82}Kr+^{40}Ca reactions at 5.5 MeV/A incident energy. Kinetic energy distributions and angular distributions of fragments with atomic number 6≤Z≤28 were measured using the 4π-INDRA array. Global features are compatible with an emission from a long-lived system. The yields around the symmetric splitting are about 30% smaller for the neutron rich system. The persistence of strong structural effects is evidenced from elemental cross-sections of the light fragments. The cross-sections for odd-Z fragments are higher for the neutron rich CN while cross-sections for even-Z fragments are higher for the neutron poor CN. Calculations assuming two different potential energy surfaces are presented.

1 Introduction

The properties of nuclear systems formed in heavy ion collisions (HIC) are under vigourous experimental and theoretical studies. Thanks to a large bombarding energy range, HIC are undoubtedly the appropriate way to explore the response of nuclei under extreme conditions (temperature, density, angular momentum, neutron richness or deformation) and to delineate the degrees of freedom at work in various perturbation regimes. Collisions at incident energies around the Coulomb barrier is well-adapted to form compound nuclei (CN) in a controlled way in terms of excitation energy and angular momentum. It has been widely reported that the decay channels of such excited nuclei involve the whole range of mass asymmetry: emission of light particles; fission process; production of intermediate mass fragments (IMFs). The competition between these decay modes is mainly ruled by the temperature and the angular momentum transferred into the emitting system in one side, and by the topology of the potential energy surface of the relevant collective degrees of freedom in the other side. The thermal and collective properties of nuclei involve fundamental nuclear quantities as level density, fission barriers and viscosity. The neutron richness (N/Z) of the nuclear system is expected to play a role on these quantities. In this contribution, we present new data on IMFs emission and fission mechanism in ^{78,82}Kr+^{40}Ca reactions at 5.5 MeV/A incident energy.

2 Experimental results

The ^{78,82}Kr+^{40}Ca reactions at 5.5 MeV/A were studied at the GANIL facility. Self-supporting 1mg/cm^2 thick ^{40}Ca targets were used. The kinetic energy and atomic number of the ejectiles were measured using the 4π-INDRA array [1]. The experimental data discussed here are based on the charged products emitted in the range $3° \leq \theta_{lab} \leq 45°$. Thanks to the reverse kinematics, the subtended angles covers roughly the forward hemisphere in the centre-of-mass (c.o.m) of the reaction. In the range $3° \leq \theta_{lab} \leq 45°$ each detection module comprises three layers: an ionization chamber (IC), a silicon detector (Si) followed with a CsI scintillator. The energy calibration was obtained using alpha particles emitted from a Cf source and from elastically scattered projectiles selected with the CIME cyclotron. The

[a] e-mail: ademard@ganil.fr

atomic charge numbers of the detected products were deduced from the energy deposited in the IC and Si detectors.

The kinetic energy distribution of the fragments is obtained from the measured energy, corrected for the energy losses in the target and in the dead zones of the IC and Si detectors. The transformation into the c.o.m frame is obtained by performing an event-by-event analysis. Fragments produced in both reactions show similar features. Fig. 1 (top panel) presents some examples of the c.o.m kinetic energy distributions of fragments produced in the ^{78}Kr+^{40}Ca reaction. Such a distribution is at variance with a temperature driven phenomenon in which a Maxwell-like energy spectra is expected. Indeed, a Gaussian-like distribution (dashed lines in top panel of Fig. 1) reproduces rather well the experimental data. For each species, the c.o.m average velocity $< V_{cm} >$ is deduced from the average kinetic energy assuming a mass number given by an empirical formula [2]. $< V_{cm} >$ is roughly independent of the emission angle and agrees with the Viola systematic [3] on total kinetic energy releases in fission process. These features indicate a strong degree of relaxation before the formation mechanism of the observed fragments and an emission dominated by the Coulomb interaction. The Coulomb origin of the process is also supported by the quasi-linear decrease of $< V_{cm} >$ with increasing charge Z. Fluctuations of the interaction barriers and emission of particles along the path to scission would explain the width of the kinetic energy distributions. It is worth noticing that for fragments with atomic numbers around Z=36, two components are clearly observed in the energy spectra, one corresponding to quasi-elastic or deep inelastic collisions. Instead of applying a procedure to unfold the various components of the spectra we prefer to consider the products with Z≤28 which are populated with only one mechanism. Moreover, Li, Be and B fragments punch-through the silicon detectors and their characteristics will be presented in forthcoming publication.

The absolute differential cross-sections $d\sigma/d\Omega_{cm}$ are deduced from the normalization with respect to the elastic scattering at forward angles which is given by the Rutherford scattering, as it is expected at 5.5 MeV/A. Fig. 1 (bottom panel) shows some exemples of angular distributions $d\sigma/d\Omega_{cm}$ for fragments measured in the ^{78}Kr+^{40}Ca reaction. Since the experiment was performed in reverse kinematics, the products associated to a fast break-up of the lighter partner is expected to be ejected in the backward hemisphere of the c.o.m, while those coming from the projectile would be strongly focused in the forward angles. In contrast with these behaviours, the measured fragment angular distributions are compatible with a $1/\sin\theta_{cm}$ dependence (dashed lines in bottom panel of Fig. 1). This feature signs a loss of memory of the beam direction as expected for a long-lived system.

To check the binary nature of the fragment formation mechanism, an event-by-event analysis is performed to extract the two biggest fragments Z_1 and Z_2 with $Z_1 \geq Z_2$ imposing $Z_1, Z_2 \geq 6$. A linear correlation between the charges of the two biggest fragments is observed, that illustrates the binary nature of the mechanism. Final states comprising three heavy fragments are marginal.

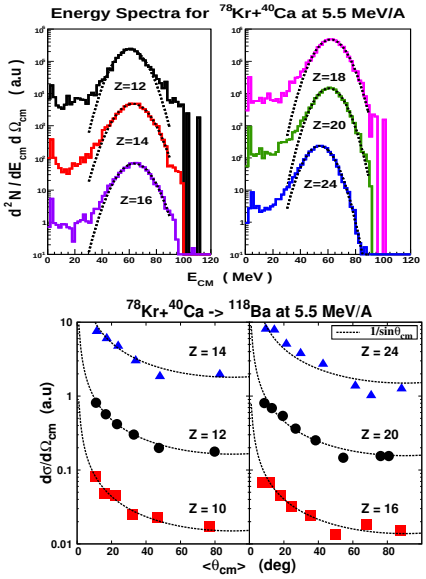

Fig. 1. (Top): Centre-of-mass kinetic energy distributions of fragments with atomic charge number Z=12, 14, 16, 18, 20, 24 produced in the ^{78}Kr+^{40}Ca reaction. Dashed lines are fits with a Gaussian function; (Bottom): Angular distributions of fragments with atomic charge number Z=10, 12, 14, 16, 20, 24 produced in the ^{78}Kr+^{40}Ca reaction. Dashed lines are fits using a $1/\sin\theta_{cm}$ function.

The inclusive cross-sections of fragments with atomic number 6≤Z≤28 are shown in the left panel of Fig. 2 for the ^{78}Kr+^{40}Ca (full squares) and for the ^{82}Kr+^{40}Ca (empty squares). The cross-section distributions of both systems exhibit a maximum around Z=28 that corresponds to half of the available charge. This indicates that these elements come either from the symmetric fission of a compound nucleus or from a class of collisions in which a full relaxation of the entrance channel mass asymmetry is reached. For fragments with Z≤10 a strong odd-even staggering of the cross-sections is visible, and this effect is still present for higher Z with a smaller amplitude. Besides these common trends, some peculiar behaviours seem to be linked to the neutron richness of the emitting system. The yields around the symmetric splitting are about 30% smaller for the neutron rich system. According to the liquid drop model, the fission barrier of a neutron poor CN is smaller than for the neutron rich one. Since the cross-section depends on the thermal energy left once the collective energy is subtracted, a higher cross-section is expected for the symmetric fission from a ^{118}Ba CN.

The influence of the neutron excess is also seen in the yields of the light fragments. The cross-sections for odd-Z fragments are higher for the neutron rich CN while cross-sections for even-Z fragments are higher for the neutron poor CN. To quantify this effect, the Z-dependence of the ratio R= $\sigma_Z^{118Ba}/\sigma_Z^{122Ba}$ is reported on the right panel of Fig. 2. The ratio R decreases roughly from 1.25 for Z=6 down to 0.75 for Z=7. For odd-Z (triangles), the ratio increases up to Z=21 and reaches a kind of plateau. For even-Z (squares), R decreases from Z=6 to Z=10 and then in-

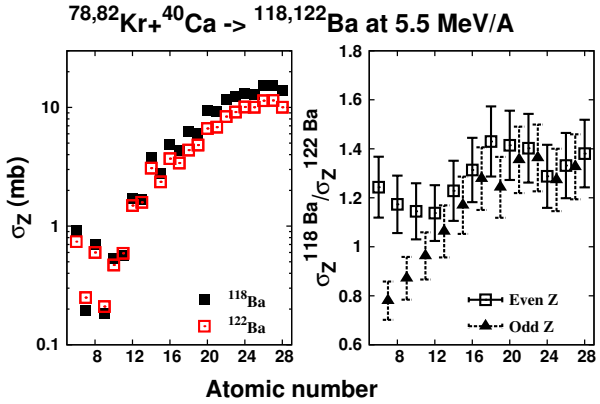

Fig. 2. Left panel: Experimental cross sections for fragments emitted in ^{78}Kr+^{40}Ca (full squares) and ^{82}Kr+^{40}Ca (empty squares) reactions; Right panel: Experimental ratio $\sigma_Z^{118Ba}/\sigma_Z^{122Ba}$ for odd-Z fragments (triangles) and even-Z fragments (squares)

creases to reach the same kind of plateau as for odd-Z. The excitation energy and the maximum angular momentum stored in the intermediate system are expected to be very similar in both reactions. Thus, the effects are probably linked to the role of the N/Z degree of freedom. Fluctuations in cross sections have already been observed in a wide range of reactions [4], [5]. For example the sensitivity to the neutron content of the emitter is reported in [5] for the ^{78,82,86}Kr+^{12}C but at variance with our data, the ratio R $\sigma_Z^{90Mo}/\sigma_Z^{98Mo}$ does not show a different behaviour for odd and even-Z. This could be due to the influence of the angular momentum which would induce different compactness of the scission configurations and thus a sensitivity to structural effects in shape degrees of freedom. Moreover, it is worth noticing that our measured Z-distributions are very close to those measured in systems prepared in similar way in terms of excitation energy and angular momentum [6]. This common features in the yields of light fragments would indicate that the even-odd staggering is not mainly driven by the structural properties of the heavy complementary partner which are different for each systems.

To summarize, our data shows the coexistence of gross features that presumably reflect the influence of the angular momentum, and a staggering behaviour that signs the persistence of structural effects (more likely pairing or shell closure) in the binary decays. These complex behaviours would be challenging for models aiming to describe the decaying mechanisms of excited nuclear systems.

The total fusion cross-sections σ_{fus} are important input ingredients for the models since they provide some clues on the initial spin distributions of the compound nuclei. In the medium-mass range, σ_{fus} is dominated by the evaporation residue component. In the present work, the (ER) component is identified thanks to the signals deposited in the IC and Si detectors. Absolute values of $d\sigma_{ER}/d\Omega_{lab}$ are deduced from the normalization with respect to the elastic scattering. Since $d\sigma_{ER}/d\Omega_{lab} \approx exp - k\theta_{lab}^2$, the experimental distribution is extrapolated towards the beam direction, and σ_{ER} could be extracted. Extensive simulations using statistical code PACE4 [7] were performed to check this procedure. The total fusion cross-sections are obtained by summing-up σ_{ER} and the yields of the fragments with charge atomic number 6≤Z≤28. We obtain σ_{fus}= 640 mb (670 mb) for the ^{78}Kr+^{40}Ca (^{82}Kr+^{40}Ca) reaction respectively. The contribution from 3≤Z≤5 is expected to not exceed few tenth of mb. The systematic error introduced by the extrapolation procedure does not allow to associate the difference in σ_{fus} to the neutron richness in the entrance channel. Last, assuming a spin distribution given by the sharp cut-off approximation we obtain J_{max} = 65$\hbar$ (67$\hbar$) for the ^{78}Kr+^{40}Ca (^{82}Kr+^{40}Ca) reaction respectively. These values are in agreement with the experimental data accumulated for similar systems.

3 Comparison with models

In this section, experimental results are compared to the statistical disintegration of an initial source and to the prediction of a model assuming the initial entrance channel as starting point. Statistical decay calculations were performed using the GEMINI code [8]. All decay channels are calculated within the Hauser-Feshbach model for Z≤2 and the transition state formalism for Z≥3. The fragment emission is ruled by the conditional saddle configuration and thermal properties. The saddle conditional energy for different mass (or charge) asymmetry is deduced from the rotating liquid drop model including finite range effects [9]. Fermi gas framework is assumed for the theoretical modelling of nuclear level density.

Dotted lines in top left (right) panels of Fig. 3 show the predictions for the disintegration of ^{118}Ba (^{122}Ba) nucleus respectively. As input ingredients, we used a sharp cut-off for the angular momentum distribution with J_{max} = 65$\hbar$ and a=A/8.5 for the level density parameter. The model reproduces well the yields around Z=28. However, the calculation overestimates the light fragments yields and the width of the Z distribution. Same results are obtained for the disintegration of the ^{122}Ba compound nucleus and the model reproduces the decreasing of the yields around the symmetry. Predicted values of the ratio $\sigma_Z^{118Ba}/\sigma_Z^{122Ba}$ are shown in the bottom panels of Fig. 3 (dotted line). The calculations reproduce qualitatively the experimental data for light fragments with odd-Z (right panel) and for Z≥14 but strongly underestimate the ratio $\sigma_Z^{118Ba}/\sigma_Z^{122Ba}$ for light even-Z fragments (bottom left panel).

Coming back to the width of the calculated Z distribution, it would be premature to conclude on the failure of the Sierk's barrier as main source of the disagreement. Indeed, some calculations describing the time evolution of the system on potential energy surface by means of the Langevin's approach indicate the sensitivity of the width to the viscosity [10]. Consequently, the test of the barrier profile as a function of the mass-asymmetry will require further experimental and theoretical investigations [11].

The dinuclear system (DNS) model [12,13] describes the time evolution of the interacting system in the mass asymmetry degree of freedom. The DNS is formed during the initial stage of the reaction when the kinetic energy

is transformed into excitation energy into the partners, and then the DNS evolves by a diffusion process along the mass asymmetry degree of freedom.The model treats the competition between the fusion and the quasi-fission processes and has been successfully compared to data involving massive nuclei. In Fig. 3 are shown the DNS results for the charge distributions (continuous lines in top panels). The improvement with respect to the transition state model is spectacular. The model predicts an even-odd staggering of the cross-sections and its decreasing as the atomic number increases. Maxima in the charge yields arise from minima in the driving potential and are caused by structure effects in the dinuclear system. Moreover, the calculated charge distribution agrees with the experimental data, and the relative yields between large asymmetry and symmetric fission is well reproduced in both reactions even though the model underestimates the yields around Z=20, that is presumably due to the influence of the shell closure. Since the calculations use the experimental masses, the disagreement would signs the fading out of the shell closure with deformation. It is worth noting that the even-odd staggering of the light fragment yields is larger in the model for both reactions. This is probably due to the experimental masse values which are included in the calculation of the driving potential and would suggest the need for an attenuation of the structural effects during the separation process. The influence of the N/Z degree of freedom of the nuclear system is illustrated in the bottom panels of Fig. 3 that show the calculated ratio $\sigma_Z^{118Ba}/\sigma_Z^{122Ba}$ for even (left panel) and odd (right panel) Z respectively. The model does not reproduce the trends of the experimental ratio. The origin of such a discrepancy is under investigation, but at first glance, it indicates the subtle interplay between microscopic properties and shape evolution of nuclei in the separation phase.

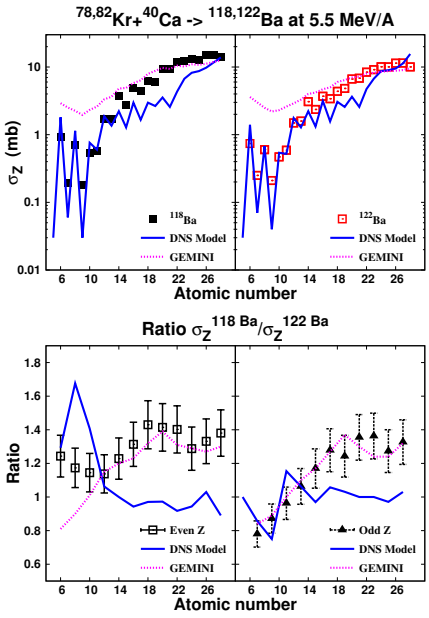

Fig. 3. Comparison with the predictions of the GEMINI (dotted lines) and DNS-Model (continuous lines). Top left (right): model predictions of the charge distribution compared to data for ^{78}Kr (^{82}Kr)+^{40}Ca reaction respectively. Bottom left (right): model predictions of the ratio $\sigma_Z^{118Ba}/\sigma_Z^{122Ba}$ for even (odd) Z respectively.

4 Conclusion

The influence of the neutron richness on binary decays was investigated in ^{78,82}Kr+^{40}Ca reactions at 5.5 MeV/A incident energy. Experimental features of the fragments were shown to be compatible with a disintegration process of a long-lived system. Persistence of structural effects that reflects the N/Z ratio of the nuclear system were evidenced from elemental cross-sections. Comparisons with models suggest the strong influence of structural effects during the separation phase in asymmetric fission. Further investigations are foreseen to study quantitatively the light particle emission during the fission process, and to identify the nuclear properties (pairing, shell closure, deformation, ...) responsible of the even-odd staggering of the light fragment yields.

5 Aknowledgments

The authors are thankful to G.G. Adamian, N. Antonenko and Sh.A. Kalandarov for showing their interest in this work. Special thanks are due to Sh.A. Kalandarov for performing the DNS calculations.This work has been supported by the Région Basse-Normandie under the contract 08P00792.

References

1. J. Pouthas *et al.*, *Nucl. Instrum. Methods Phys. Res.* **A357**, (1995) 418
2. R.J. Charity *et al.*, *Nucl. Phys.* **A476**, (1988) 516
3. C. Beck *et al.*, *Phys. Rev.* **C53**, (1996) 1989
4. S. Steinhauser *et al.*, *Nucl. Phys.* **A634**, (1988) 516; Sl. Cavallaro *et al.*, *Phys. Rev.* **C57**, (1996) 731; M.V. Ricciardi *et al.*, *Nucl. Phys.* **A733**, (2004) 299
5. K.X. Jing *et al.*, *Nucl. Phys.* **A645**, (1999) 203; T.S. Fan *et al.*, *Nucl. Phys.* **A679**, (2000) 121
6. L.G. Sobotka *et al.*, *Phys. Rev.* **C36**, (1987) 2713; J. Boger *et al.*, *Phys. Rev.* **C50**, (1994) 1006
7. O. Tarasov, www.nscl.msu.edu/tarasov/lise.html
8. R.J. Charity *et al.*, *Nucl. Phys.* **A483**, (1988) 43
9. A.J. Sierk, *Phys. Rev.* **C33**, (1986) 2039
10. P.N. Nadtochy, *Phys. Rev.* **C75**, (2007) 064614
11. J.P. Wieleczko *et al.*, New aspects of Heavy ion Collisions Near the Coulomb Barrier, FUSION08, AIP Conference Proceedings Vol. 1098
12. G.G. Adamian *et al.*, *Nucl. Phys.* **A618**, (1997) 176; G.G. Adamian *et al.*, *Phys. Rev.* **C68**, (2003) 034601
13. Sh.A. Kalandarov *et al.*, proceedings of the International Conference on Nuclear Structure and Related Topics, NSRT2009, Dubna, Russia